Carbohydrate Research 343 (2008) 2657–2666

Contents lists available at ScienceDirect

Carbohydrate Research

journal homepage: www.elsevier.com/locate/carres

Effect of gelatin on molecular mobility in amorphous sucrose detected by erythrosin B phosphorescence

Yumin You, Richard D. Ludescher *

Department of Food Science, Rutgers, The State University of New Jersey, 65 Dudley Road, New Brunswick, NJ 08901-8520, United States

ARTICLE INFO

Article history:
Received 24 June 2008
Received in revised form 22 July 2008
Accepted 7 August 2008
Available online 12 August 2008

Keywords:
Amorphous solid
Phosphorescence
Molecular mobility
Sucrose
Gelatin
Dynamic heterogeneity

ABSTRACT

We have used phosphorescence from the triplet probe erythrosin B (Ery B) to evaluate the effect of gelatin on the molecular mobility of the amorphous sucrose matrix as a function of temperature. Ery B was dispersed in amorphous sucrose and sucrose–gelatin films at ratios of ~1:10^4 (probe/sucrose), and delayed emission spectra and emission decay transients were measured over the temperature range from 5 to 100 °C. Analysis of spectra using a lognormal function provided the peak energy and bandwidth of the emission. The emission peak frequency decreased at low (0.00022–0.0007) gelatin concentrations and increased at high (above 0.0022) gelatin concentrations, indicating that gelatin increased the extent, and thus the rate, of dipolar relaxation at low gelatin content and decreased the extent at higher gelatin content. Decay transients were well fit to a stretched exponential function at all gelatin contents and temperatures. Analysis of the emission lifetimes provided a measure of the rate of non-radiative decay to the ground state, an indicator of matrix molecular mobility. This rate increased at low (0.00022–0.0022) and decreased at high (>0.0073) gelatin wt ratios. Analysis of the effect of gelatin on the emission bandwidth, the stretching exponent β, and the variation of lifetime across the emission band indicated that matrix dynamic site heterogeneity increased at low and decreased at high gelatin wt ratios. These results provide a novel insight into the complex dynamic effects of the gelatin polymer on the molecular mobility of the amorphous sucrose matrix.

© 2008 Elsevier Ltd. All rights reserved.

1. Introduction

Sucrose glasses act as cryoprotective agents during anhydrobiosis, are a component of many solid foods, and provide the matrix of boiled sweets. The ability of sucrose to protect biomaterials from freeze-thaw damage and provide long-term storage stability has attracted both mechanistic studies and efforts to develop solid-state formulations for labile compounds in foods and in pharmaceuticals.

Two main mechanisms, glass dynamics and specific interaction, are proposed to understand the role of sucrose in the stabilization of sensitive compounds during dehydration and storage.[1,2] The glass dynamics mechanism focuses on the rigid, inert matrix formed upon the vitrification of stabilizers such as sugars.[3,4] By forming into amorphous, non-crystalline solids upon rapid drying from aqueous solution or cooling from the melt, sugars change from soft, pliable, and flexible matrixes at high temperature to hard, brittle, and rigid matrixes at low temperature. This change results from an enormous increase in viscosity due to the nonlinear decrease in the rate of translational as well as rotational and vibrational mobility with decrease in temperature or solvent.[5] Since glass formation is a kinetic process, stability is expected to correlate to changes in molecular mobility in the rigid matrix.

The specific interaction mechanism, commonly applied to understand protein stabilization, states that stabilizers form hydrogen bonds at specific sites with target compounds.[6–8] These hydrogen bonds help to maintain the native structure and the spatial integrity of the compound after water is removed, and consequently enhance stability. Sucrose is thus a nearly ideal matrix material for stabilization since it is both a good glass former and a good hydrogen bonder. For better functionality and long-term stability, however, formulation design tends to select sucrose glasses mixed with other compounds ranging from small molecules such as salts to macromolecules such as hydrocolloids.

Molecular mobility within amorphous solids is usually manifest in relaxation processes. Amorphous solids exhibit a glass transition at a temperature (T_g) that reflects the onset of large-scale molecular motions (α-relaxations) that underlie translational and whole molecule rotational motions. They also typically exhibit a secondary transition at a temperature ($T_\beta < T_g$) that reflects the onset of localized molecular motions (β-relaxations) linked to localized whole molecule or segmental motions. The temperature-dependent molecular mobility controls physical and chemical properties by modulating the nature, rates, and extents of reactions that occur during processing and storage of biomaterials. Hydrocolloids are

* Corresponding author. Tel.: +1 732 932 9611x231; fax: +1 732 932 6776.
E-mail address: ludescher@aesop.rutgers.edu (R. D. Ludescher).

0008-6215/$ - see front matter © 2008 Elsevier Ltd. All rights reserved.
doi:10.1016/j.carres.2008.08.009

often selected to stabilize formulations due to high solution viscosities and solid state T_g's far above the storage temperature (ambient or below).

Gelatin, a product of the structural and chemical degradation of collagen, is perhaps the most frequently used hydrocolloid in the food, pharmaceutical, and photographic industries.[9] Recently, edible gelatin films have attracted considerable interest due to their functional properties as well as their importance as an appropriate model for studying the behavior of amorphous biopolymers in the solid state.[10] Many studies have focused on the phase transition of gelatin[10–14] and the thermal and mechanical properties of gelatin films under the influence of plasticizers and large molecular weight carbohydrates.[15–21]

Gelatin can form a variety of supermolecular structures, depending on the casting temperature and time, the initial concentration in the gelatin solution, the nature of the solvent and coexisting compounds, and other factors.[22] These structures, which reflect the ability of gelatin polymers to aggregate into locally ordered triple helices, modulate the physico-chemical and mechanical properties of the gelatin films. Cold-cast gelatin films, spread at room temperature and lower, have an entangled network with a variable number of triple helical cross-links that contribute to the macroscopic stability and strength of gelatin films.[23] Hot-cast films, spread from aqueous solutions at temperature above 35 °C, have no cross-links and are assumed to have the conformation of a statistical coil.[22] Lukasik and Ludescher found that the matrix mobility (both the extent of matrix relaxation and matrix collisional quenching rates) was higher in cold-cast (cross-linked) than hot-cast (not cross-linked) films.[24] Since little information is available on the relationship between triple helix formation and matrix mobility, hot-cast gelatin films which do not form cross-links were used for the present study to simplify data interpretation.

So far as we are aware, most previous studies have focused on the stabilization of protein by sugars in protein-based solid systems[25,26,10] or on the stability of protein entrapped in a sugar matrix.[2,27] There is little information in the literature on the effect of biopolymers on the properties of the sugar matrix. The measurement of molecular mobility of amorphous sugars at low levels of macromolecules will provide insight into the mechanism by which the biopolymer modulates sucrose matrix mobility. In previous studies, we have used erythrosin B phosphorescence to monitor the molecular mobility as well as dynamic site heterogeneity in amorphous solid sucrose[28] and in sucrose containing NaCl.[29] In the present study, phosphorescence of Ery B was used to measure the matrix mobility in thin films composed of amorphous sucrose-gelatin mixtures. Gelatin content was varied from 0.00022 to 0.365 (g gelatin/g sucrose) by addition of gelatin to the concentrated sucrose solution prior to film formation. The temperature dependence of mobility was measured and analyzed at different gelatin contents, generating families of mobility versus temperature curves that reveal a complex, concentration-dependent effect of gelatin on sucrose matrix mobility.

2. Results

At a probe/sucrose mole ratio of $1{:}10^4$, each Ery B molecule is surrounded by a matrix shell ~10–11 sucrose molecules thick. At this concentration, Ery B does not aggregate and thus provides information on the mobility of the unperturbed sucrose matrix.[30] The phosphorescence spectra of Ery B in 66% sucrose solution and in gelatin solution (100 mg/mL) show emission peaks at the same position, suggesting no extensive binding of the probe to gelatin.

Data collected from phosphorescence measurements in sucrose–gelatin films prepared from three different drying methods (drying under a heat gun, on a hot plate, and freeze drying) were almost the same, indicating that the physical state and properties of the films were nearly identical. Data presented here were collected from films prepared by drying under a heat gun. This similarity also indicates that the films contained the minimum residual moisture content and that the remaining water could not be removed under these experimental conditions. The fairly high moisture content in a pure gelatin film (~5 wt %) was probably overestimated using the gravimetric method due to the hydrophilic nature of gelatin.

2.1. Delayed emission spectra

The delayed emission spectra of erythrosin B in amorphous sucrose and sucrose–gelatin films at a dye/sucrose mole ratio of $1{:}10^4$ displayed a longer wavelength phosphorescence band (maximum ~680 nm) due to emission from the triplet state T_1 and a shorter wavelength delayed fluorescence band (maximum ~555 nm) due to emission from the singlet state S_1 repopulated by thermally stimulated reverse intersystem crossing from T_1.[31] Delayed emission spectra of amorphous sucrose films and films with various gelatin weight ratios collected over the temperature range from 5 to 100 °C showed a decrease in phosphorescence (I_P) and an increase in delayed fluorescence (I_{DF}) intensity with increasing temperature (data not shown). Both emission bands shifted to longer wavelength at high temperature. The intensity ratio was analyzed as a van't Hoff plot of $\ln(I_{DF}/I_P)$ versus $1/T$, and the linear slope was used to estimate the energy gap (ΔE_{TS}) between the triplet and singlet states (Eq 6; Section 5). In amorphous sucrose and gelatin, the values of ΔE_{TS} were 31.56 ± 0.56 and 33.62 ± 0.52 kJ mol^{-1}, respectively. In sucrose films with gelatin weight ratios of 0.00022, 0.00073, 0.0022, 0.0073, 0.022, 0.073, and 0.365, the values of ΔE_{TS} were 32.41 ± 0.40, 32.34 ± 0.26, 31.74 ± 0.60, 31.54 ± 0.21, 31.37 ± 0.43, 31.81 ± 0.48, and 32.40 ± 0.31 kJ mol^{-1}, respectively.

The peak frequency (ν_p) and bandwidth (Γ) for both delayed fluorescence and phosphorescence emission were determined by fitting to a log-normal line shape function (Eqs 1 and 2; Section 5); ν_p for phosphorescence is plotted in Figure 1. The decrease in emission energy reflects an increase in the average extent of dipolar relaxation around the excited triplet state prior to emission.[32,28] The phosphorescence peak frequency in pure sucrose decreased gradually and linearly at low temperature ($R^2 = 0.9932$ for a linear fit) and then more steeply at higher temperature ($R^2 = 0.9596$). This biphasic behavior reflects the influence of the glass transition on the peak frequency.[28,33,34] The phosphorescence peak frequency in pure gelatin, on the other hand, decreased linearly and gradually over the entire temperature range ($R^2 = 0.9992$). The total decrease in frequency with temperature was much smaller in gelatin (177 cm^{-1}) than in sucrose (338 cm^{-1}), with most of the additional decrease occurring above 60 °C. The variation of frequency with temperature in sucrose–gelatin mixtures was intermediate between that seen in pure sucrose and in pure gelatin, with curves at low concentration exhibiting biphasic behavior and those at higher concentration displaying more linear monotonic decreases with temperature.

The complex effect of gelatin on the Ery B peak frequency at each temperature is illustrated in Figure 2. The peak frequency was lower in sucrose–gelatin than that in pure sucrose at wt ratios of 0.00022 and 0.00073 and higher at wt ratios of 0.022 and above. Although the magnitude of the decrease or increase varied with temperature, the fractional change was nearly constant over the temperature range from 5 to 65 °C and showed more dramatic decreases at low concentration and increases at high concentration at higher temperatures.

The phosphorescence bandwidth reflects the extent of inhomogeneous broadening due to a range of interactions between the

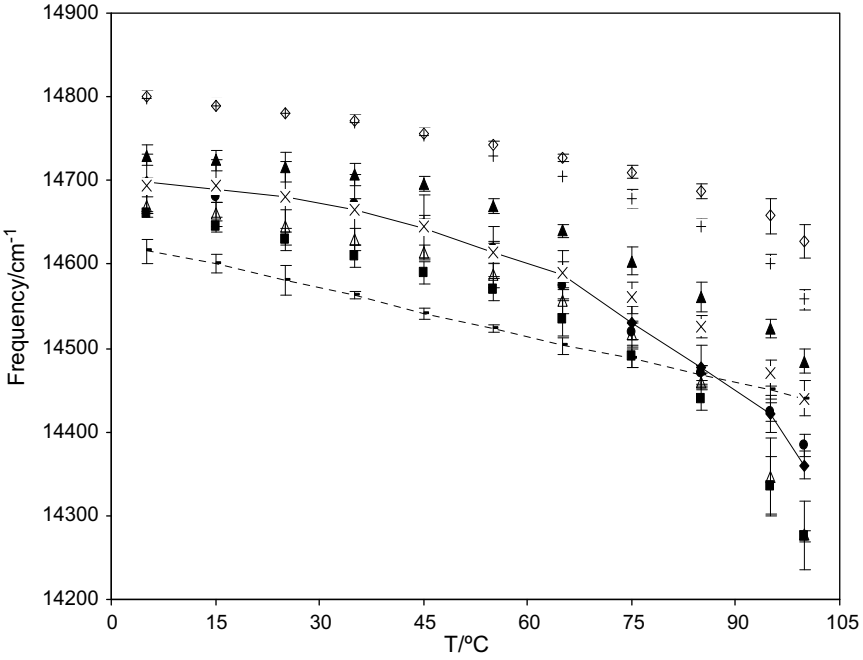

Figure 1. Peak frequency (ν_p) for phosphorescence emission from erythrosin B in amorphous sucrose–gelatin films as a function of temperature. Films were composed of sucrose (♦), gelatin in sucrose at wt ratios of 0.00022 (■), 0.00073 (△), 0.0022 (●), 0.0073 (×), 0.022 (▲), 0.073 (+), 0.365 (◇), and gelatin (–).

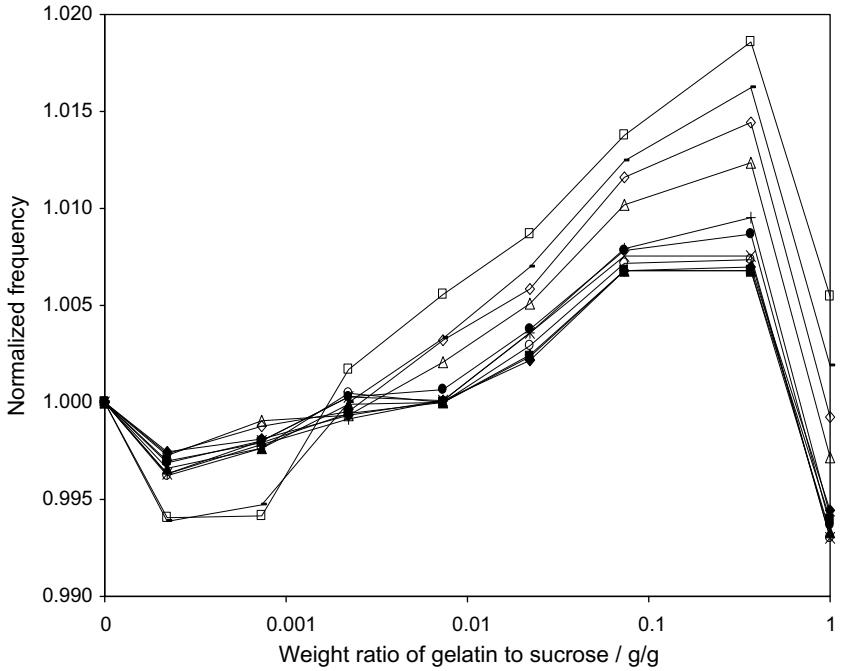

Figure 2. Peak frequency, normalized at each temperature to the value in pure sucrose, for phosphorescence emission from erythrosin B in amorphous sucrose–gelatin films as a function of weight ratio of gelatin/sucrose over the temperature range from 5 to 100 °C. Spectra were collected at 5 °C (♦), 15 °C (■), 25 °C (▲), 35 °C (○), 45 °C (×), 55 °C (●), 65 °C (+), 75 °C (△), 85 °C (◇), 95 °C (–), and 100 °C (□).

matrix and the excited probe. The phosphorescence bandwidth increased gradually at low and more steeply at high temperature (data not shown) indicating a corresponding increase in the range of energetically distinct matrix environments in the amorphous matrix. Amorphous sucrose, sucrose films with different gelatin contents, and pure gelatin exhibited essentially similar trends over the whole temperature range.

2.2. Phosphorescence decay kinetics

Phosphorescence intensity decays were measured over the temperature range from 5 to 100 °C in amorphous films; all decays were well fit to a stretched exponential decay model.[28,33] The stretched exponential lifetimes and stretching exponents (β) are plotted as a function of temperature in Figure 3. The lifetimes

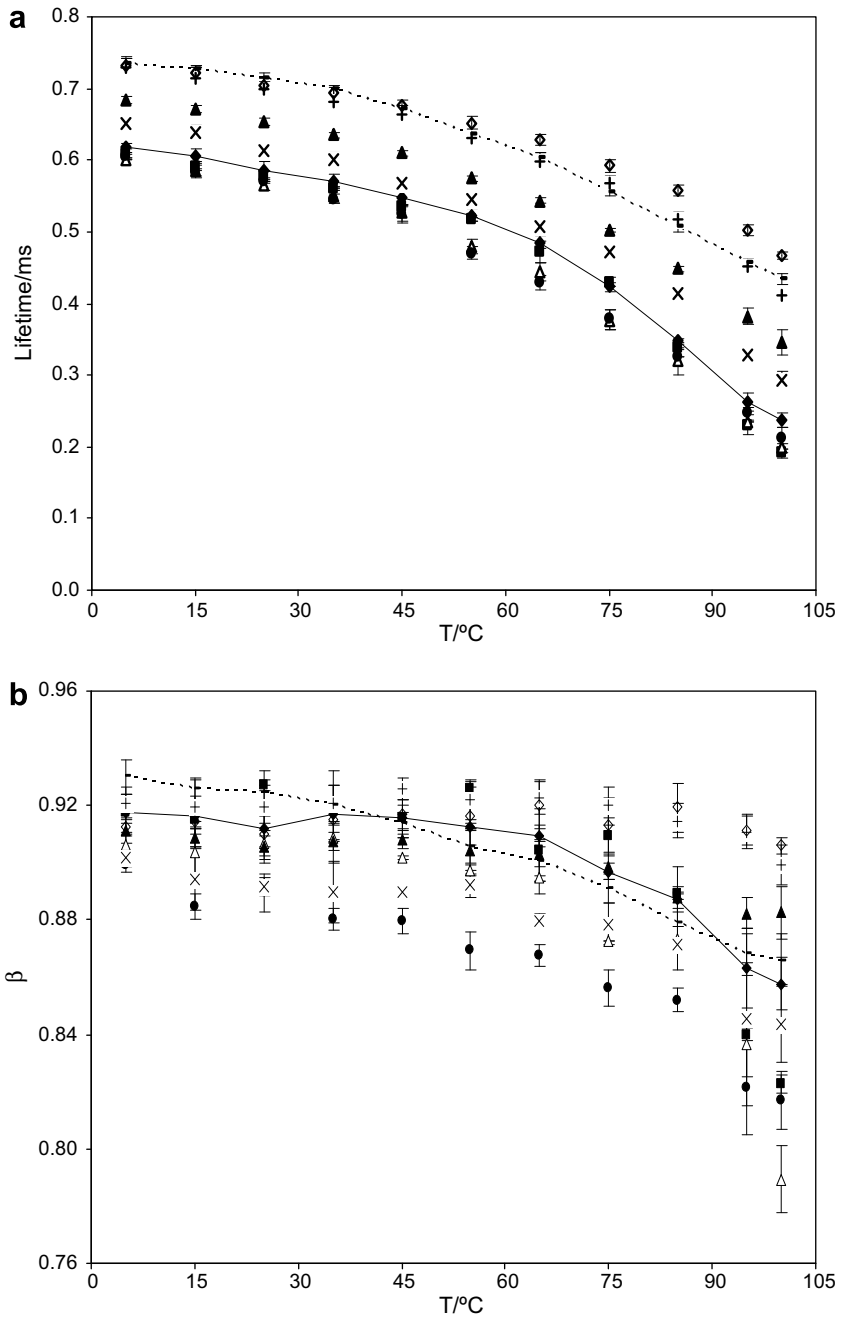

Figure 3. Temperature dependence of (a) lifetime and (b) stretching exponent β obtained from fits to a stretched exponential decay model of the intensity decay of erythrosin B in amorphous sucrose films. Films were composed of sucrose (♦), gelatin in sucrose at wt ratios of 0.00022 (■), 0.00073 (△), 0.0022 (●), 0.0073 (×), 0.022 (▲), 0.073 (+), 0.365 (◇), and gelatin (–).

decreased biphasically with increasing temperature, exhibiting a gradual linear decrease at low and a more dramatic decrease at high temperature. A similar thermal profile was seen in sucrose, gelatin, and in all sucrose–gelatin mixtures. Lifetimes decreased slightly, but significantly, below those seen in pure sucrose at low gelatin wt ratios and increased considerably at gelatin wt ratios of 0.0073 and higher. The stretching exponent β, a measure of the width of the distribution of lifetimes required to fit the intensity decay,[35] was approximately constant up to ~60 °C and decreased, in general, at higher temperature in sucrose, sucrose–gelatin, and gelatin films (Fig. 3b).

The decrease in lifetime with temperature reflects an increase in the rate of non-radiative decay of the excited triplet state T_1 due to an increase in both the rate of non-radiative decay to the ground state S_0 (k_{TS0}) and the rate of reverse intersystem crossing to the first excited singlet state S_1 (k_{TS1}).[36,28] Based on the maximum physically reasonable value of k_{TS1},[28] an estimate of the lower limit of k_{TS0} was calculated as described in Section 5 (Eq 4); these values are plotted as $\ln(k_{TS0})$ versus $1/T$ in Figure 4. The non-radiative quenching rate k_{TS0} was approximately constant at low temperature and increased dramatically at high temperature in sucrose, indicating that this rate is sensitive to modes of molecular mobility thermally activated at T_g.[28] The extent of the increase in k_{TS0} at high temperature, however, decreased as the concentration of gelatin increased until k_{TS0} was approximately constant across the entire temperature range at gelatin wt ratios of 0.073 and above (but not in pure gelatin).

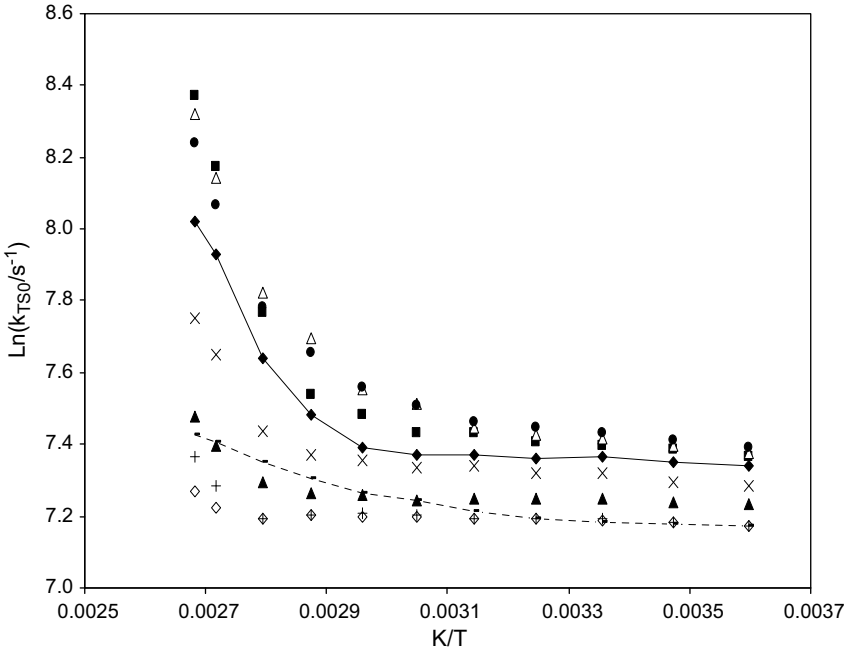

Figure 4. Arrhenius plot of the effect of temperature on the rate constant for non-radiative decay (k_{TS0}) of the erythrosin B triplet state T_1 to the singlet ground state S_0; rates calculated from the lifetime data of Figure 3a (see text for additional details). Films were composed of sucrose (♦), gelatin in sucrose at wt ratios of 0.00022 (■), 0.00073 (△), 0.0022 (●), 0.0073 (×), 0.022 (▲), 0.073 (+), 0.365 (◇), and gelatin (–).

The gelatin concentration dependence of k_{TS0} is plotted in Figure 5. The magnitude of k_{TS0} increased at low concentration (wt ratios from 0.00022 to 0.0022) and decreased at high concentration of gelatin (wt ratios of 0.0073 and above) compared to the value in pure sucrose. The fractional increase in k_{TS0} seen at low concentration of gelatin varied with temperature, being moderate at 45 °C and below, and more dramatic and temperature dependent at 55 °C and above. The fractional decrease in k_{TS0} seen at high concentration of gelatin also varied with temperature, being moderate and essentially constant with temperature at 65 °C and below, and more dramatic and temperature dependent at 75 °C and above. The maximum fractional decrease at high concentration was slightly larger than the maximum fractional increase at low concentration gelatin. The value of k_{TS0} in pure gelatin was lower than that in sucrose at each temperature.

2.3. Spectral heterogeneity

Phosphorescence intensity decays of Ery B in films with different gelatin contents were measured as a function of excitation

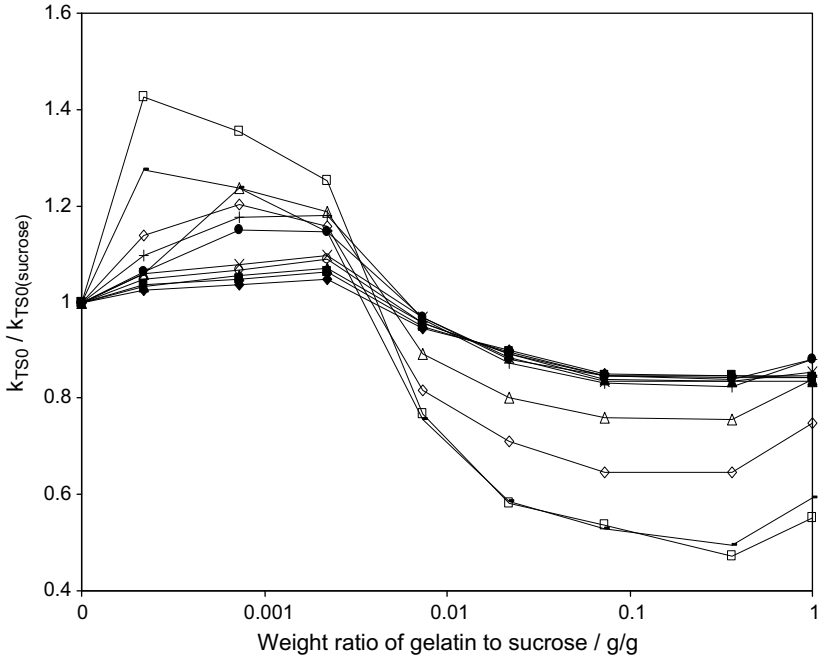

Figure 5. The effect of gelatin content on the rate k_{TS0} normalized at each temperature to the value in pure sucrose. Data were collected at 5 °C (♦), 15 °C (■), 25 °C (▲), 35 °C (○), 45 °C (×), 55 °C (●), 65 °C (+), 75 °C (△), 85 °C (◇), 95 °C (–), and 100 °C (□).

and emission wavelengths at 25 °C; all decay transients were well fit using a stretched exponential decay model. The triplet quenching rate k_{TS0}, calculated from these lifetimes, is plotted versus excitation and emission wavelengths at different gelatin wt ratios in Figure 6a. The rate k_{TS0} increased with increasing emission wavelength in all films. The quenching rate was slightly larger in gelatin than in sucrose at low wt ratios ($\leqslant$0.00073) but decreased significantly at higher gelatin content. At wt ratio of 0.073, k_{TS0} varied from 1240 s^{-1} at 640 nm to 1540 s^{-1} at 720 nm, much lower than the values of 1410 s^{-1} and 1780 s^{-1} seen at the same wavelengths in pure sucrose. The quenching rate also varied systematically across the excitation band. In sucrose, k_{TS0} was lowest at 530 nm and higher at the blue and red edges of the excitation band. In the presence of gelatin, k_{TS0} was higher at low (wt ratio $\leqslant$0.00073) and lower at higher gelatin content than in sucrose. At low gelatin content, the variation in the quenching rate across both emission and excitation bands was similar to that in the sucrose matrix. Increasing gelatin concentration diminished the variation in the quenching rate across both the emission and the excitation bands.

The stretching exponent β also varied as a function of both excitation and emission wavelengths (Fig. 6b). In sucrose and sucrose–gelatin films, β was lower at the blue edge of the emission band, increased with increasing wavelength to a maximum at 680–690 nm, and then decreased slightly at the red edge. The values of β were slightly lower in the presence of gelatin. The variation

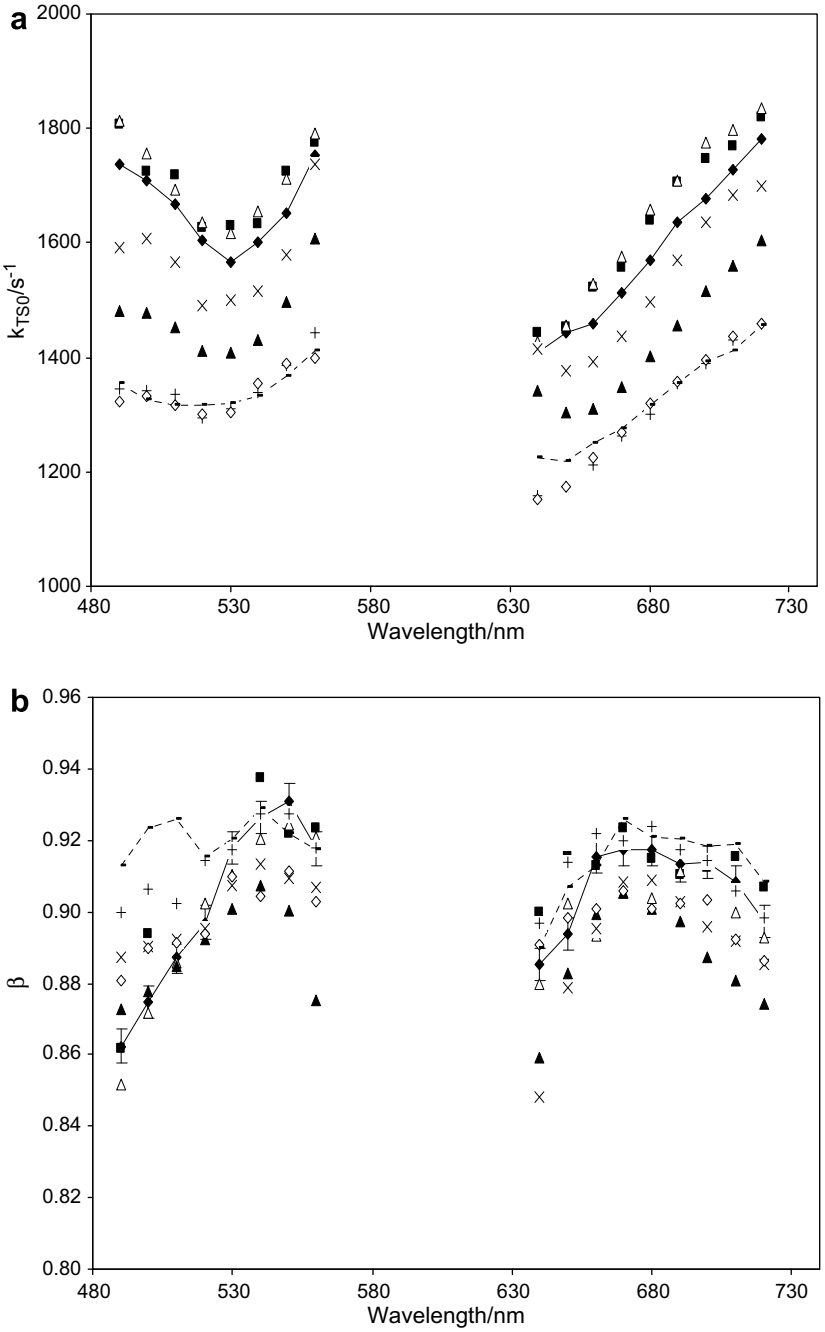

Figure 6. The effect of excitation (with 680 nm emission) and emission wavelengths (with 530 nm excitation) on the rate constants for non-radiative decay of the erythrosin B triplet state (k_{TS0}) (a) and stretching exponents β (b) from fits of erythrosin B phosphorescence intensity decays to the stretched exponential decay model. Data are from films composed of sucrose (♦), gelatin in sucrose at wt ratios of 0.00022 (■), 0.00073 (△), 0.0073 (×), 0.022 (▲), 0.073 (+), 0.365 (◇), and gelatin (–).

of β across the excitation band in sucrose-gelatin films was similar to that seen in sucrose.

3. Discussion

The phosphorescence emission energy and lifetime (intensity) of Ery B in amorphous solids are mainly influenced by two kinds of matrix molecular mobility: dipolar relaxation that affects the emission energy of the triplet state and collisional quenching that increases the rate of non-radiative decay of the triplet state.[28,33,37] Our discussion of the effect of gelatin on amorphous sucrose is based on an analysis of how the emission energy and lifetime of Ery B are modulated by these two modes of matrix molecular mobility. Since the shape of the emission spectra was not affected by the addition of gelatin, we conclude that Ery B did not aggregate in the presence of gelatin and thus accurately reports matrix properties.[30]

3.1. Matrix molecular mobility

The Ery B emission energy provides a sensitive measure of the average extent of dipolar relaxation around the triplet state during its excited state lifetime.[38,32] Over a temperature increase of 95 °C, the probe emission energy decreased significantly in both pure sucrose and sucrose–gelatin mixtures. This decrease reflects the mobility of sugar hydroxyl groups, either due to localized β-relaxations in the glass or due to larger-scale α-relaxations activated at T_g.[28] The total decrease in emission energy over the measured temperature range decreased as the concentration of gelatin increased, apparently due to modulation of the glass transition and consequent suppression of α-relaxations in the mixtures.

The effect of gelatin on the emission energy was complex, decreasing the energy at low gelatin concentration (wt ratios from 0.00022 to 0.00073) and increasing the energy at higher concentration (wt ratios of 0.022 and above) compared to pure sucrose (Fig. 2). Since the triplet lifetime actually decreased at low gelatin concentration (Fig. 3a), thus shortening the time window for dipolar relaxation, this decrease in emission energy provides strong, albeit indirect, evidence that the rate of dipolar relaxation increased significantly at low gelatin content. By a similar argument, since the excited state lifetime actually increased at higher gelatin content, the increase in emission energy provides strong indirect evidence that the rate of dipolar relaxation decreased significantly at higher gelatin content.

The emission lifetime of Ery B is directly modulated by the rate of radiative emission k_{RP}, the rate of reverse intersystem crossing to the excited triplet state k_{TS1}, and the rate of intersystem crossing to the ground state k_{TS0}. The rate of radiative emission is constant[39] and equal to 41 s^{-1} in Ery B,[40] while k_{TS1} varies with temperature in an Arrhenius fashion.[40,41] The rate of intersystem crossing k_{TS0} is modulated by the physical state of the amorphous matrix;[36,28] it reflects both the manner in which the excited T_1 state is vibrationally coupled to the ground state S_0 and the manner in which the ground state vibrational energy can dissipate into the surrounding matrix. Since the efficiency of this vibrational dissipation is related to the overall mobility of the matrix, k_{TS0} provides a direct measure of matrix mobility.[42]

The variation of k_{TS0} with temperature thus provides a measure of the effect of temperature on the matrix mobility (Fig. 4). The increase in k_{TS0} reflects the activation of cooperative α-relaxations at the glass transition in sucrose which more effectively quench the Ery B triple state.[28,33,34] The temperature of the transition can be calculated from the intersection of the trendlines at high and low temperatures in these Arrhenius plots. The transition temperatures were 76.5 °C in sucrose, and 77.9, 75.9, 77.0, 83.2, 84.5, 88.1, and 94.2 °C at wt ratios of 0.00022, 0.00073, 0.0022, 0.0073, 0.022, 0.073, and 0.365, respectively. The increase in the transition temperature indicates that addition of gelatin increased the temperature range over which the sucrose matrix retained glass-like mobility. Gelatin itself has a high glass transition temperature[43] (153 °C); the gradual increase in k_{TS0} seen in pure gelatin at higher temperatures may reflect thermal activation of local modes of motion within the glassy protein polymer. Since k_{TS0} is higher in pure gelatin than in gelatin–sucrose mixtures, the presence of sucrose appears to limit molecular mobility in the protein matrix; similar behavior has been seen in amorphous β-lactoglobulin films.[44]

Because gelatin may influence the properties of sucrose glasses by changing the glass transition temperature of sucrose, the T_g of sucrose–gelatin mixtures was estimated using the Couchman and Karasz equation[45] with T_g = 153 °C and ΔC_p = 0.5 J/g °C for gelatin.[43] Because the gelatin levels were low, calculated T_g's of mixtures were not significantly different from those of sucrose except at wt ratio of 0.365 where T_g = 83 °C. When the values of k_{TS0} were plotted on a temperature scale normalized to the individual T_g's, all the curves were similar in shape except that the curves with lower gelatin contents were slightly above and those with higher gelatin contents were significantly below the sucrose curve (data not shown). This suggests that gelatin influenced the sucrose matrix both by slightly increasing T_g and by directly modulating the overall mobility through specific interactions between sucrose and gelatin.

3.2. Dynamic site heterogeneity

Research using a variety of spectroscopic techniques indicates that supercooled liquids and amorphous solids exhibit both spatial and temporal dynamic heterogeneity, as the matrix mobility varies through space at any given time and through time at any given site.[46,47] This physical model is also consistent with extensive evidence from Ery B phosphorescence. Spectral heterogeneity in Ery B has been observed in a wide variety of amorphous sugars and sugar alcohols,[28,48,49] and globular and fibrous proteins,[37,50,51] indicating that dynamic site heterogeneity may be a characteristic feature of amorphous biomaterials.

In the amorphous sucrose matrix, Ery B is distributed among dynamically distinct sites with different emission energies and matrix quenching rates.[28] The variation of phosphorescence lifetime with emission wavelength reflects a variation in the rate constant k_{TS0} for deexcitation of the triplet state. This variation reflects a distribution of local matrix sites that vary in terms of their overall molecular mobility.[28] Probes in 'blue-shifted' sites with slow dipolar relaxation have longer lifetimes due to smaller values of k_{TS0}; these sites are thus less mobile. Probes in 'red-shifted' sites with fast rates of dipolar relaxation have shorter lifetimes due to larger values of k_{TS0}; these sites are thus more mobile. The variation in k_{TS0} with emission wavelength (Fig. 6a) was larger at low gelatin level and smaller at high gelatin level compared with sucrose, suggesting increased dynamic heterogeneity at low gelatin levels but decreased heterogeneity at higher gelatin levels. The values of the stretching exponent β were comparably lower in sucrose–gelatin than in pure sucrose across the emission band (Fig. 6b), indicating a broader distribution of dynamic environments and thus a decreased ability within these sites to dynamically average out spectroscopic differences.

The temperature dependence shows that the stretching exponent was lower than pure sucrose in the presence of small amounts of gelatin but higher at gelatin content above 0.073 wt ratio (Fig. 3b), indicating a broader distribution of dynamic environments (more site heterogeneity) at low and a narrower distribution (less site heterogeneity) at higher gelatin content. And finally, the emission bandwidth (Γ, FWHM) increased slightly with the

addition of small amounts of gelatin and decreased at wt ratios of 0.073 and above (data not shown), indicating that the distribution of site energies was slightly broader than pure sucrose at low and slightly narrower at high gelatin levels.

A number of independent spectroscopic measures thus indicate that the sucrose matrix with low concentrations of gelatin has both increased rates of molecular mobility and increased extent of dynamic site heterogeneity; the sucrose matrix with low concentrations of gelatin is thus both more mobile and more dynamically heterogeneous than sucrose. On the other hand, the sucrose matrix with higher concentrations of gelatin has both decreased rates of molecular mobility and decreased extent of dynamic site heterogeneity; the sucrose matrix with higher concentrations of gelatin is thus both less mobile and less dynamically heterogeneous than sucrose.

3.3. Interactions between sucrose and gelatin

The contrasting dynamic effects of gelatin occurred in radically different concentration regimes. The decrease in mobility occurred at gelatin wt ratios of ~0.01 and above, concentrations sufficiently high to modulate bulk properties in solution (form elastic gels, e.g.). At a wt ratio of 0.01, the mole ratio of amino acid residues to sucrose is ~0.037, calculated based on an average residue molecular weight of 93 g/mol;[58–60] each amino acid residue in the gelatin polymer was thus able to restrict the mobility of approximately 27 sucrose molecules (1/0.037). The increase in mobility, on the other hand, was manifest at gelatin wt ratios as low as 0.0001 (mole ratio 0.00037), indicating that each amino acid residue of gelatin was able to increase the mobility of approximately 2700 sucrose molecules; this implies a perturbed solvent shell ~29 molecules thick along the length of the extended polymer chain. (Assuming that sucrose molecules are perturbed radially around each amino acid residue in the extended polymer chain.)

It is possible that the probe Ery B does not sample the bulk properties of the matrix but rather preferentially partitions to the polymer surface; if this interface were more mobile than the bulk matrix, then the probe would report increased molecular mobility even at very low gelatin concentrations. However, it is difficult to understand how increasing gelatin concentration above ~0.003 wt fraction would reverse the trend and decrease the mobility, as one would expect more extensive partitioning onto the gelatin surface, and thus enhanced mobility, at higher gelatin concentrations. Instead, the data clearly indicate that gelatin, at concentrations sufficiently high to directly modulate bulk properties, caused a decrease in matrix mobility. Studies of the effect of amylose starch or xanthan gum on sucrose mobility indicated that these unrelated polymers also increased matrix mobility at low and decreased matrix mobility at high wt ratios in a manner nearly identical to that seen with gelatin.[52]

Plasticization by water also does not appear to explain these results. Although the moisture content increased with gelatin concentration (data summarized in Section 5), the moisture content was insignificant at low gelatin concentration and only increased above 1 wt % under conditions (high gelatin concentration) where the mobility actually decreased.

We thus conclude that the complex dynamic behavior described here reflects a true effect of the hydrocolloid gelatin polymer on the mobility of the amorphous sucrose matrix.

The decrease in mobility at ~0.01 wt ratio of gelatin and above is consistent with dynamic rheology studies of sugar/gelatin mixtures,[53–56] which indicate that addition of only 1 wt % polymer increases both the viscous and elastic moduli as well as the glass transition temperature of the sugar matrix. Our data suggest that addition of gelatin increases the temperature of the dynamic transition by perhaps as much as 15–20 °C at high gelatin content. Although we see no evidence for it in our results, it is also possible that the dynamic behavior at high wt ratios also reflects phase separation into sugar-rich and gelatin-rich domains as noted by Kasapis et al.[55] Spectroscopic measurements appear to reflect not only the bulk effects of gelatin polymer on matrix dynamics at high wt ratios but also to monitor some more local and subtle effect on matrix dynamics at low wt ratios.

The pure sucrose matrix is a hydrogen-bonded network. This network is the major determinate of molecular packing and matrix rigidity. Small amounts of the gelatin polymer may interfere with the formation of this hydrogen-bonding network for several reasons: gelatin contains significantly fewer hydrogen-bonding sites and many non-polar groups which cannot hydrogen bond; hydrogen-bonding groups in gelatin differ in chemical structure and thus strength from those in sucrose; and gelatin is a large polymer with conformational constraints that limit its ability to form a strong and well-ordered hydrogen-bonded network. Since films were prepared from aqueous solutions at ~50 °C, well above the melting temperature of the triple helix, gelatin molecules are assumed to have the conformation of a statistical coil.[22] At low gelatin wt ratios where contacts between random coil gelatin and sucrose are most likely, the presence of gelatin may disrupt the cooperative sucrose hydrogen-bonding network, generating more loosely packed regions with higher mobility and greater dynamic heterogeneity compared to pure sucrose.

4. Conclusion

Both composition and temperature modulate the molecular mobility of amorphous solids. Based on analysis of the phosphorescence emission energy and lifetime of Ery B in sucrose and sucrose-gelatin films over the temperature range from 5 °C to 100 °C, we conclude that gelatin exerts a strong, dose-dependent effect on the molecular mobility of amorphous sucrose. The emission energy decreased and k_{TS0} increased at wt ratios below ~0.0073, indicating that low concentrations of gelatin increased the mobility of the sucrose matrix. On the other hand, the emission energy increased and k_{TS0} decreased at wt ratios above ~0.0073, indicating that higher concentrations of gelatin decreased the mobility of the sucrose matrix. Spectral heterogeneity in the Ery B phosphorescence supports a physical model of dynamic site heterogeneity within amorphous sucrose above and below the glass transition temperature. Addition of gelatin at low wt ratio increased and at higher wt ratio decreased the extent of dynamic heterogeneity. These data thus provide dramatic insight into the complex dynamic effects of gelatin on the molecular mobility of the amorphous sucrose matrix.

5. Experimental

5.1. Preparation of amorphous films

We prepared glassy sucrose films by using a slightly modified version of our published method[28] in which 20–40 μm thick films are prepared by casting from aq solns. We prepared gelatin stock soln, using VEE GEE Superclear Type A 300 bloom pigskin gelatin obtained from Vyse Gelatin Co. (Schiller Park, IL), using a slightly modified version of our previous method.[57]

Pure gelatin films were prepared from 100 mg/mL aq gelatin soln containing a dye content of $\sim 5.6 \times 10^{-5}$ mol dye/mol residues. Calculations were made assuming an average residue molecular weight of 93 g/mol, calculated from the relative abundance of each amino acid in acid-processed porcine skin gelatin.[58–60] This mole ratio was selected in order to produce tractable films under

established conditions; the amount of dye was sufficient to provide adequate signal/noise in spectroscopic measurements. It is assumed that at this low level of dispersing, ~56 dye molecules per million residues, the physical properties of the resultant films are unaffected. The mixture was stirred and heated above 65 °C until a clear soln was obtained. The soln was pipetted in 15 μL aliquots onto quartz slides. The following procedure applied to make a glassy gelatin film was the same as that applied to make a pure sucrose film.

Gelatin–sucrose solns were prepared from sucrose soln containing dye at $1:10^4$ (dye/sucrose mole ratio). Gelatin soln was added to the sucrose solns to obtain a series of mixtures with gelatin/sucrose weight ratios of 0.00022, 0.00073, 0.0022, 0.0073, 0.022, 0.073, and 0.365, respectively. Prior to preparing glassy films, sucrose–gelatin solns were filtered through a membrane with 0.2 μm pores. The procedure applied to make a sucrose-gelatin film was the same as that applied to make a pure sucrose film.

Gelatin–sucrose films were dried using heat gun for 10 min. The films were also dehydrated on a hot plate and by vacuum-drying; the cast films were either dried in contact with a heated plate at ~65 °C for 20 min, or dried under a pressure of 1 kPa for at least 24 h at 55 °C.

5.2. Moisture measurements

Water content in amorphous films was determined gravimetrically by measuring the difference in mass before and after drying for 24 h at 70 °C in an Ephortee (Haake Buchler, Inc.) vacuum oven at 1 kPa. Sample films were scratched from quartz slides and ground into powders in a glove box containing P_2O_5 and Drie-Rite with a relative humidity less than 5%. Pure sucrose and pure gelatin films contained 0.56 ± 0.13 and 4.78 ± 0.35 wt % water, respectively, while gelatin-sucrose samples contained 0.63 ± 0.02 (gelatin/sucrose wt ratio 0.00022), 0.95 ± 0.14 (wt ratio 0.00073), 0.78 ± 0.20 (wt ratio 0.0022), 0.82 ± 0.15 (wt ratio 0.0073), 0.98 ± 0.26 (wt ratio 0.022), 1.38 ± 0.01 (wt ratio 0.073), and 1.52 ± 0.15 (wt ratio 0.365) wt % water.

5.3. Luminescence measurements

Luminescence measurements were made using a Cary Eclipse Fluorescence spectrophotometer (Varian Instruments, Walnut Creek, CA). Prior to any phosphorescence measurements, all samples were flushed for at least 15 min with nitrogen gas which contained less than 1 ppm oxygen to eliminate oxygen quenching. At each target temperature samples were equilibrated for 1 min/°C increase in temperature. The temperature was controlled using a thermo-electric temperature controller (Varian Instruments, Walnut Creek, CA). To eliminate moisture condensation during the measurements below room temperature, dry air was used to flush the chamber surrounding the cuvette holder. All the measurements were made at least in triplicate.

Delayed fluorescence and phosphorescence emission spectra were collected from 520 to 750 nm (10 nm bandwidth) at 1 nm intervals using excitation of 500 nm (20 nm bandwidth) over a temperature range from 5 to 100 °C with an observation window of 5.0 ms and an initial delay time of 0.2 ms to suppress fluorescence coincident with the lamp pulse. Emission spectra from sucrose or sucrose–gelatin films without probe were subtracted from each spectrum although the signal of background was very low.

The energy of the emission maximum (ν_p) and the full width at half maximum (FWHM) of the emission band was determined by using a log-normal line-shape function[61] to fit both delayed fluorescence and phosphorescence.

$$I(\nu) = I_0 \exp\left\{-\ln(2)\left(\frac{\ln[1+2b(\nu-\nu_p)/\Delta]}{b}\right)^2\right\} \quad (1)$$

where I_0 is the maximum emission intensity, ν_p is the peak frequency (cm^{-1}), Δ is a linewidth parameter, and b is an asymmetry parameter. The bandwidth (FWHM; Γ) was calculated according to the following equation:

$$\Gamma = \Delta\left(\frac{\sinh(b)}{b}\right) \quad (2)$$

For delayed luminescence spectra collected from 520 to 750 nm, a sum of log-normal functions for delayed fluorescence ($I_{df}(\nu)$) and phosphorescence ($I_p(\nu)$) was used to fit the spectra. Each emission band was fit to independent parameters.

For lifetime measurements as a function of temperature, samples were excited at 530 nm (20 nm bandwidth) and emission transients collected at 680 nm (20 nm bandwidth) over the temperature range from 5 to 100 °C. Phosphorescence intensity decays were collected over a window of 5 ms with an initial delay of 0.1 ms and increments of 0.04 ms. Each decay was the average of 20 cycles. Because intensity decays were complex, a stretched exponential, or Kohlrausch–Williams–Watts, decay function was selected to analyze the intensity decay:[38,62,28]

$$I(t) = I_0 \exp(-(t/\tau)^{\beta}) + \text{constant} \quad (3)$$

where I_0 is the initial amplitude, τ is the stretched exponential lifetime, and β is an exponent varying from 0 to 1 and characterizing the distribution of lifetimes.[35] The use of a stretched exponential model provides a direct measurement of a continuous distribution of lifetimes, which is appropriate for describing a complex glass possessing a distribution of relaxation times for the dynamic molecular processes. The smaller the β value, the more non-exponential the intensity decay and the broader the distribution of lifetimes. The program NFIT (Galveston, TX) was used to fit the decay; goodness of fit was evaluated by examining χ^2 and R^2. Plots of modified residuals (defined as the difference between the intensity from the fit decay curve and the measured intensity divided by the square root of the measured intensity) were also used as an indicator of the goodness of fit. R^2 for all fits ranged from 0.99 to 1.00 and modified residuals plots fluctuated randomly around zero amplitude.

Phosphorescence decay transients of Ery B as a function of emission wavelength were measured with excitation wavelength at 530 nm (20 nm bandwidth); emission wavelength varied from 640 to 720 nm (20 nm bandwidth). Phosphorescence decay transients as a function of excitation wavelength were measured with emission wavelength at 680 nm (20 nm bandwidth); excitation wavelength ranged from 490 to 560 nm (20 nm bandwidth). These experiments were performed at 25 °C.

5.4. Photophysical scheme

Our analysis of the delayed emission is similar to the photophysical scheme for erythrosin B outlined by Duchowicz et al.[40] The measured emission rate for phosphorescence (k_p) is the sum of all possible deexcitation rates for the triplet state T_1:

$$\tau^{-1} = k_P = k_{RP} + k_{TS1} + k_{TS0} + k_Q[Q] \quad (4)$$

In this equation, k_{RP} is the rate of radiative emission to the ground state S_0. For erythrosin B, k_{RP} is 41 s^{-1} and constant with temperature;[40] k_{TS1} is the rate of thermally activated reverse intersystem crossing from the triplet state T_1 to the singlet state S_1. The value can be estimated from the Arrhenius equation:

$$k_{TS1}(T) = k^o_{TS1} \exp(-\Delta E_{TS}/RT) \quad (5)$$

where k^{o}_{TS1} is the maximum rate of intersystem crossing from T_1 to S_1 at high temperature, ΔE_{TS} is the energy gap between T_1 and S_1, $R = 8.314\ J\ K^{-1}\ mol^{-1}$, and T is the temperature in Kelvin. The value of ΔE_{TS} is calculated from the slope of a Van't Hoff plot of the natural logarithm of the ratio of intensity of delayed fluorescence (I_{DF}) to phosphorescence (I_P):

$$d[\ln(I_{DF}/I_P)]/d(1/T) = -\Delta E_{TS}/R \quad (6)$$

where I_{DF} and I_P are the maximum intensity values determined from analysis of the delayed emission bands as described above. The value of k_{TS1} at 25 °C was estimated as $88\ s^{-1}$, using $k^{0}_{TS1} = 3.0 \times 10^{7}\ s^{-1}$ and $\Delta E_{TS} = 31.56$ kJ/mol.[28] (Due to our method of analyzing the photophysical rate constants which potentially overestimates k_{TS1}, our reported values of k_{TS0} may actually underestimate the true value of k_{TS0}.[28])

In the presence of oxygen, the quenching rate $k_Q[Q]$ is the product of rate constant k_Q and the oxygen concentration $[O_2]$. By flushing nitrogen throughout the measurements, we assume that no oxygen quenching occurred. One of the non-radiative decay routes is through intersystem crossing to the ground state S_0. The decay rate is expressed by $k_{TS0,}$ which reflects the rate of collisional quenching of the probe due to both internal and external factors.[36] We assume that the term k_{TS0} primarily reflects the external environmental factors since the self collisional quenching among probe molecules can be neglected within the extremely viscous amorphous solid. In this study, temperature-dependent term k_{TS0} can be calculated by difference from Eq 4.

References

1. Kets, E. P. W.; Ijpelaar, P. J.; Hoekstra, F. A.; Vromans, H. *Cryobiology* **2004**, *48*, 46–54.
2. Chang, L.; Shepherd, D.; Sun, J.; Ouellette, D.; Grant, K. L.; Tang, X.; Pikal, M. J. *J. Pharm. Sci.* **2005**, *94*, 1427–1444.
3. Franks, F.; Hatley, R. H. M.; Mathias, S. F. *BioPharm.* **1991**, *4*, 38. 40-42, 55.
4. Slade, L.; Levine, H. *Crit. Rev. Food Sci. Nutr.* **1991**, *30*, 115–360.
5. Zallen, R. *The Physics of Amorphous Solids*; John Wiley & Sons: New York, 1983. pp 1–32.
6. Carpenter, J. F.; Crowe, J. H. *Biochemistry* **1989**, *28*, 3916–3922.
7. Carpenter, J. F.; Prestrelski, S. J.; Arakawa, T. *Arch. Biochem. Biophys.* **1993**, *303*, 456–464.
8. Crowe, J. H.; Crowe, L. M.; Carpenter, J. F. *BioPharm.* **1993**, *6*, 28–29. 32–33.
9. Wood, P. D. In *The Science and Technology of Gelatin*; Ward, A. G., Courts, A., Eds.; Academic Press: New York, 1977; pp 414–437.
10. D'Cruz, N. M.; Bell, L. N. *J. Food Sci.* **2005**, *70*, E64–E68.
11. Marshall, A. S.; Petrie, S. E. B. *J. Photogr. Sci.* **1980**, *28*, 128–134.
12. Slade, L.; Levine, H. In *Advances in Meat Research: Collagen as a Food*; Pearson, A. M., Dutson, T. R., Bailey, A. J., Eds.; AVI/Van Nostrand Reinhold: New York, 1987; Vol. 4, pp 251–266.
13. Sobral, P. J. A.; Habitante, A. M. Q. B. *Food Hydrocolloids* **2001**, *15*, 377–382.
14. Kasapis, S.; Sablani, S. S. *Int. J. Biol. Macromol.* **2005**, *36*, 71–78.
15. Pinhas, M. F.; Blanshard, J. M. V.; Derbyshire, W.; Mitchell, J. R. *J. Therm. Anal.* **1996**, *47*, 1499–1511.
16. Sablani, S. S.; Kasapis, S.; Al-Rahbi, Y.; Al-Mugheiry, M. *Drying Technol.* **2002**, *20*, 2081–2092.
17. Sobral, P. J. A.; Menegalli, F. C.; Hubinger, M. D.; Roques, M. A. *Food Hydrocolloids* **2001**, *15*, 423–432.
18. Vanin, F. M.; Sobral, P. J. A.; Menegalli, F. C.; Carvalho, R. A.; Habitante, A. M. Q. B. *Food Hydrocolloids* **2005**, *19*, 899–907.
19. Arvanitoyannis, I.; Nakayama, A.; Aiba, S. *Carbohydr. Polym.* **1998**, *36*, 105–119.
20. Arvanitoyannis, I.; Nakayama, A.; Aiba, S. *Carbohydr. Polym.* **1998**, *37*, 371–382.
21. Arvanitoyannis, I.; Psomiadou, E.; Nakayama, A.; Aiba, S.; Yamamoto, N. *Food Chem.* **1997**, *60*, 593–604.
22. Kozlov, P. V.; Burdygina, G. I. *Polymer* **1983**, *24*, 651–666.
23. Menegalli, F. C.; Sobral, P. J. A.; Roques, M. A.; Laurent, S. *Drying Technol.* **1999**, *17*, 1697–1706.
24. Lukasik, K. V.; Ludescher, R. D. *Food Hydrocolloids* **2006**, *20*, 96–105.
25. Tzannis, S. T.; Prestrelski, S. J. *J. Pharm. Sci.* **1999**, *88*, 360–370.
26. Chinachoti, P.; Steinberg, M. P. *J. Food Sci.* **1988**, *53*, 932–934.
27. Wright, W. W.; Guffanti, G. T.; Vanderkooi, J. M. *Biophys. J.* **2003**, *85*, 1980–1995.
28. Pravinata, L. C.; You, Y.; Ludescher, R. D. *Biophys. J.* **2005**, *88*, 3551–3561.
29. You, Y.; Ludescher, R. D. *Carbohydr. Res.* **2008**, *343*, 350–363.
30. You, Y.; Ludescher, R. D. *Appl. Spectrosc.* **2006**, *60*, 813–819.
31. Parker, C. A. *Photoluminescence of Solution*; Elsevier Publishing: Amsterdam, 1968. pp 320–321.
32. Lakowicz, J. R. *Principles of Fluorescence Spectroscopy*, 3rd ed.; Plenum Press: New York, 2006.
33. Shirke, S.; Takhistov, P.; Ludescher, R. D. *J. Phys. Chem. B* **2005**, *109*, 16119–16126.
34. Shirke, S.; Ludescher, R. D. *Carbohydr. Res.* **2005**, *340*, 2654–2660.
35. Lindsey, C. P.; Patterson, G. D. *J. Chem. Phys.* **1980**, *73*, 3348–3357.
36. Papp, S.; Vanderkooi, J. M. *Photochem. Photobiol.* **1989**, *49*, 775–784.
37. Nack, T. J.; Ludescher, R. D. *Food Biophys.* **2006**, *1*, 151–162.
38. Richert, R. *J. Chem. Phys.* **2000**, *113*, 8404–8429.
39. Turro, N. J. *Modern Molecular Photochemistry*; University Science Books: Mill Valley, CA, 1991.
40. Duchowicz, R.; Ferrer, M. L.; Acuna, A. U. *Photochem. Photobiol.* **1998**, *68*, 494–501.
41. Lettinga, M. P.; Zuilhof, H.; van Zandvoort, A. M. J. *Phys. Chem. Chem. Phys.* **2000**, *2*, 3697–3707.
42. Fischer, C. J.; Gafni, A.; Steele, D. G.; Schauerte, J. A. *J. Am. Chem. Soc.* **2002**, *124*, 10359–10366.
43. Tsereteli, G. I.; Smirnova, O. I. *J. Therm. Anal. Calorim.* **1992**, *38*, 1189–1201.
44. Sundaresan, K. V. Ph.D. Dissertation, Rutgers University, New Brunswick, NJ, 2008.
45. Roos, Y. *Phase Transitions in Foods*; Academic Press: San Diego, 1995. pp 193–246.
46. Ediger, M. D. *Annu. Rev. Phys. Chem.* **2000**, *51*, 99–128.
47. Richert, R. *J. Phys.: Condens. Matter* **2002**, *14*, R738–R803.
48. Shirke, S.; Ludescher, R. D. *Carbohydr. Res.* **2005**, *340*, 2661–2669.
49. Shirke, S.; You, Y.; Ludescher, R. D. *Biophys. Chem.* **2006**, *123*, 122–133.
50. Lukasik, K. V.; Ludescher, R. D. *Food Hydrocolloids* **2006**, *20*, 88–95.
51. Sundaresan, K. V.; Ludescher, R. D. *Food Hydrocolloids* **2008**, *22*, 403–413.
52. You, Y. Ph.D. Dissertation, Rutgers University, New Brunswick, NJ, 2007.
53. Mitchell, J. R. In *Gums and Stabilizers for the Food Industry 10*; Williams, P. A., Phillips, G. O., Eds.; Royal Society of Chemistry: Cambridge, 2000; pp 243–254.
54. Kasapis, S.; Al-Marhoobi, I. M. A. In *Gums and Stabilizers for the Food Industry 10*; Williams, P. A., Phillips, G. O., Eds.; Royal Society of Chemistry: Cambridge, 2000; pp 303–316.
55. Kasapis, S.; Al-Marhoobi, I. M.; Deszczynski, M.; Mitchell, J. R.; Abeysekera, R. *Biomacromolecules* **2003**, *4*, 1142–1149.
56. Kasapis, S.; Mitchell, J.; Abeysekera, R.; MacNaughton, W. *Trends Food Sci. Technol.* **2004**, *15*, 298–304.
57. Simon-Lukasik, K. V.; Ludescher, R. D. *Food Hydrocolloids* **2004**, *18*, 621–630.
58. Clark, R. C.; Courts, A. In *The Science and Technology of Gelatin*; Ward, A. G., Courts, A., Eds.; Academic Press: New York, 1977; pp 209–247.
59. Eastoe, J. E.; Leach, A. A. In *The Science and Technology of Gelatin*; Ward, A. G., Courts, A., Eds.; Academic Press: New York, 1977; pp 73–107.
60. Creighton, T. E. *Proteins: Structures and Molecular Properties*, 2nd ed.; W.H. Freeman: New York, 1992.
61. Maroncelli, M.; Fleming, G. R. *J. Chem. Phys.* **1987**, *86*, 6221–6239.
62. Lee, K. C. B.; Siegel, J.; Webb, S. E. D.; Leveque-Fort, S.; Cole, M. J.; Jones, R.; Dowling, K.; Lever, M. J.; French, P. M. W. *Biophys. J.* **2001**, *81*, 1265–1274.